ChemComm

ROYAL SOCIETY OF CHEMISTRY

COMMUNICATION

View Article Online
View Journal | View Issue

Cite this: *Chem. Commun.*, 2022, **58**, 5622

Received 15th February 2022,
Accepted 11th April 2022

DOI: 10.1039/d2cc00919f

rsc.li/chemcomm

Chemical crosslinking in 'reactive' multicomponent gels†

Santanu Panja and Dave J. Adams *

We show that the hydrolysis of EDC can be used to construct a reactive system to trigger permanent covalent crosslinking between the components in multicomponent gels comprising gelators with a carboxylic acid and amine group yielding an amide functionalized gel with enhanced mechanical properties.

Supramolecular low molecular weight hydrogels are physically crosslinked polymers where small organic molecules (gelators) interact to form a self-assembled network by non-covalent interactions.[1,2] The network formed during self-assembly traps large volumes of water and so the hydrogels behave as a solid despite containing significant amounts of liquid. In recent years, most research on these gels focuses on the exploration of gels as soft, functional materials in the fields of drug delivery, cell culture, actuators, and optoelectronics.[3–6] However, one issue with these gels is that they tend to break at low strain and this limits the range of applications for which they are suitable.

To overcome these issues, different approaches have been taken. The properties can be enhanced by adding polymers.[7–9] An alternative method is to modify the noncovalent interactions between the gelator molecules by exposing gels towards stimuli like heat, pH, ions, UV-light, or chemical analytes.[10] Another approach is the stimuli-triggered chemical crosslinking of gelators that enables enhancement of mechanical properties of the materials by covalent bond formation between the components. Many methods have been applied to achieve chemical crosslinking in supramolecular gels, including photo-triggered dimerization of tyrosine and coumarin,[11,12] photopolymerization of diacetylenes,[13] oxidative disulfide formation,[14] and dynamic covalent bond formation involving crosslinking agents (such as glutaraldehyde[15] or Genipin[16]).

Typically, supramolecular gels composed of a single gelator component are subjected to crosslinking by these methods. Another interesting yet unexplored possibility is to drive a permanent covalent crosslinking between the components in multicomponent system. In recent years, multicomponent self-assembly has emerged as a powerful strategy to synthesize gels with higher tunability, adaptive and responsive properties than single component systems.[17–20] Here, we utilize carbodiimide as a chemical reagent to construct a reactive multicomponent system and thereby instigate the components to undergo crosslinking. In synthetic gel chemistry, carbodiimides are typically used as a fuel to construct transient gels through functional group modification of the component in a predetermined or programmable manner.[21–23] Of the different carbodiimides, hydration of EDC (1-ethyl-3-(3-dimethylaminopropyl)carbodiimide) into its corresponding urea is the most common method that has been applied to construct peptide-based transient gels.[23] In a typical reaction, EDC first interacts with the carboxylic acid of a peptide forming a highly reactive *O*-acylisourea intermediate (Fig. 1a).[23]

Hydrolysis of the *O*-acylisourea or reaction with a nucleophile releases the urea waste product. Recently, this concept has been

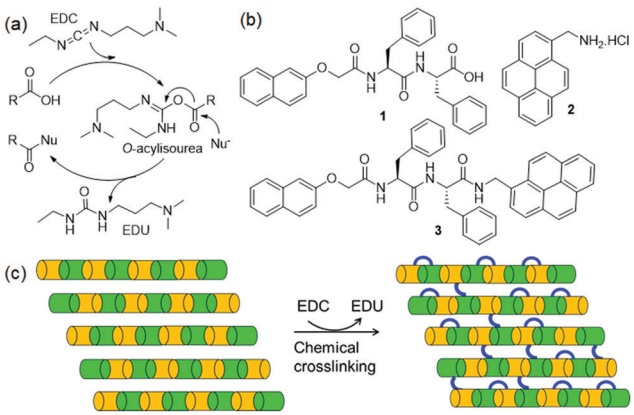

Fig. 1 (a) EDC triggered reaction cycle in presence of an acid and a nucleophile (Nu^-).[23] (b) Chemical structures of compounds **1** and **2**, and the EDC triggered cross-linking product **3**. (c) Conceptual cartoon schematic showing EDC triggered crosslinking between the components bearing a carboxylic acid and amine functionality in a multicomponent gel system. Crosslinking is possible between the adjacent fibres or between the components present in the same fibres.

School of Chemistry, University of Glasgow, Glasgow, G12 8QQ, UK.
E-mail: dave.adams@glasgow.ac.uk

† Electronic supplementary information (ESI) available. See DOI: https://doi.org/10.1039/d2cc00919f

applied to create transient covalent crosslinking *via* anhydride formation in polymeric materials.[24–26] Here we show that, with appropriate designing of the gel system, the EDC-triggered pathway can be employed to achieve a permanent covalent crosslinking between the components. To achieve this, we design a multicomponent hydrogel comprising of gelators with a carboxylic acid (**1**) and amine (**2**) functional groups (Fig. 1b). When EDC is introduced into the system, we find that depending on the pH of the medium, EDC triggered the amide bond formation (**3**) between the components yielding gels with enhanced mechanical properties (Fig. 1c).

We began with the traditional 'mixing of ionic-complementary components' to construct the basic platform of our multicomponent system.[17–20] The naphthalene dipeptide **1** (2 mg mL^{-1}) is able to form a self-supported, transparent gel in DMSO–water (pH of the gel is ~4.1) (Fig. 2a–d).[27] The pyrene-coupled ammonium salt **2** produces a free-flowing solution under similar conditions. When equimolar amounts of **1** and **2** were mixed, a turbid gel was obtained with a pH of around 3.1 (Fig. 2e). The properties of the mixed gel of (**1** + **2**) were significantly different from the single component gel of **1**. Rheological studies confirmed that the presence of **2** results in >50% reduction in the stiffness (G') of the material compared to the hydrogel of **1** alone (Fig. 2h and Fig. S1, ESI†). Confocal microscopy imaging revealed that both the single and multicomponent gels contain spherulitic domains of fibers as their microstructure (Fig. 2i and j), with a greater density of spherulitic domains in the multicomponent gel.

The changes in gel properties of **1** in the presence of **2** is due to co-assembly between the components as shown by spectroscopic studies. By UV-vis spectroscopy, the naphthalene absorption in the hydrogel of **1** at 330 nm merged with the pyrene absorption and appeared at 341 nm in the mixed gel (**1** + **2**) (Fig. S2, ESI†). The emergence of a broad peak in the region 350–375 nm in the multicomponent gel indicates a difference in the underlying molecular packing of the binary gel compared to the hydrogel of **1** alone. FTIR spectroscopy (Fig. S3, ESI†) shows that the hydrogel of **1** alone exhibited strong amide carbonyl stretching at 1647 cm^{-1} and 1695 cm^{-1} along with a broad peak at 1730 cm^{-1} corresponding to the carbonyl stretching of the carboxylic group. In the multicomponent gel, while the amide carbonyl stretches of **1** remain unaffected, the carboxylic carbonyl stretching moved to the lower region by 12 cm^{-1} and appeared at 1718 cm^{-1}. Moreover, the signatures of –OH and amide –NH stretching of **1** in the region 3300–3400 cm^{-1} became too broad to distinguish in the multicomponent gel,[28] and only a sharp signal at 3284 cm^{-1} attributing the –NH stretching of **2** became predominant. These results show co-assembly occurs in the multicomponent gel (**1** + **2**).

To drive the crosslinking between **1** and **2** in the gel, we used hydrolysis of EDC (as the hydrochloride salt) to urea to trigger the acid-amine coupling in the binary gel (**1** + **2**). We added 1 equimolar amount of EDC (with respect to **1**) on the top of the gel and allowed the system to react for ~20 h. To check the coupling reaction, the ^{1}H NMR spectrum of the EDC-treated gel was compared with the original gel of (**1** + **2**). The proton NMR of the EDC-treated gel was identical to that of the multicomponent gel (**1** + **2**) (without EDC) indicating no amide bond formation at pH 3.1 (Fig. S4, ESI†). The FTIR spectra of the gels obtained before and after the addition of EDC were also identical (Fig. S5, ESI†). No amide coupling occurs even when EDC was added directly to the mixture of (**1** + **2**) instead of post-gelation functionalization (Fig. S4, ESI†). To understand this, we added an aqueous solution of EDC to the DMSO solution of **1** present at a lower concentration and in absence of **2**. At a concentration of 0.75 mg mL^{-1}, no gelation was noticed for **1**, instead, a viscous material was formed that did not allow inversion of the vial (Fig. S6, ESI†). However, in presence of EDC, an invertible gel appeared almost instantly which collapsed after ~15 min. Similar transient gelation was achieved when compound **1** was treated with EDC in presence of equimolar amount of HCl (Fig. S6, ESI†). These observations show that compound **1** readily reacts with EDC and undergoes *O*-acylisourea formation.[23] We suggest that in the multicomponent gel at pH 3.1, compound **2** no longer acts as a nucleophile due to protonation. Simple hydrolysis of the *O*-acylisourea resulted in regeneration of compound **1** and so there was no cross-coupling product **3**.

Multicomponent gels with ionic complementary functionalities can form hierarchical structures on pH change.[29,30] Keeping in mind, we mixed components **1** and **2** in presence of different amounts of NaOH (1 and 2 molar equivalents with respect to **1**) to achieve sequential deprotonation of the components. In presence of 1 equimolar of NaOH, gelator **1** (pK_a of 5.7[27]) is expected to be deprotonated first while the addition of 2 equimolar amounts of NaOH deprotonates both **1** and **2** (pK_a 8.1, Fig. S7, ESI†). Interestingly, under both conditions, we obtained a gel with a pH of 7.8 and 10.4 respectively (Fig. 2f and g). Neither **1** or **2** alone formed a gel at high pH implying the gelation of the mixed system (**1** + **2**) at both pH 7.8 and 10.4 is again driven by co-assembly.

The mechanical properties of the co-assembled gels depend on the pH of the medium. Of the three multicomponent gels

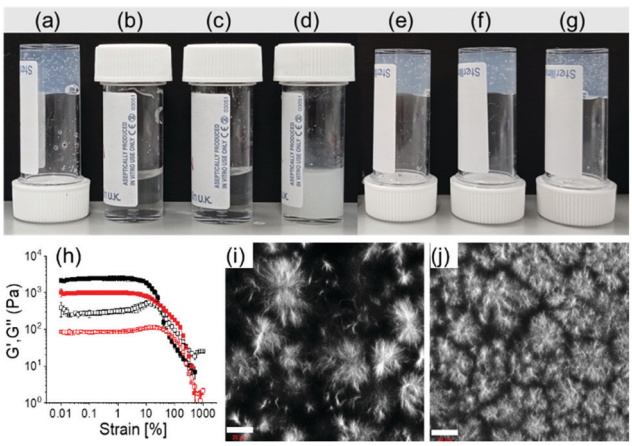

Fig. 2 (a–d) Photographs of the phase changes of **1** (a and b) and **2** (c and d) in absence (a and c) and presence (b and d) of 1 equiv. of NaOH. (e–g) Photographs of the multicomponent gels of (**1** + **2**) at pH (a) 3.1 (with no NaOH), (b) 7.8 (with 1 equiv. of NaOH and (c) 10.4 (with 2 equiv. of NaOH). (h) Strain sweep experiments of the hydrogel of **1** (black) and the multicomponent gel (**1** + **2**) (red) at pH 3.1. The closed symbols represent G′, the open symbols G″. (b) and (c) represent confocal fluorescence microscopy images (scale bars represent 20 μm) of the hydrogels **1** and (**1** + **2**) at pH 3.1 respectively. In all cases, concentration of **1** is 2 mg mL^{-1} and molar ratio of **1** and **2** is 1 : 1. Solvent is DMSO/H_2O (20/80, v/v).

(at pH 3.1, 7.8, and 10.4), the gel at pH 7.8 has the highest stiffness (storage modulus, G') (Fig. S8, ESI†). There was also a change in the microstructures of the gels at high pH. Both the gels at pH 7.8 and 10.4 showed densely packed spherical aggregates as their microstructures (Fig. S9, ESI†) in contrast to the large spherulitic domains of fibers at pH 3.1 (Fig. 2j). The differences in the microstructure as well as in mechanical properties of the gels is due to different intermolecular interactions between **1** and **2** at the different pH. On increasing the pH from 3.1 to 7.8, the amide carbonyl stretches of **1** moved from 1647 cm^{-1} and 1695 cm^{-1} to 1634 cm^{-1} and 1663 cm^{-1} respectively (Fig. S10, ESI†). On further increasing the pH to 10.4, while the peak at 1663 cm^{-1} remained unaffected the band at 1634 cm^{-1} further shifted to 1632 cm^{-1}. These results suggest the existence of different hydrogen-bonding interactions involving the amide groups at different pH. The data indicate the existence of acid–base equilibrium in the gel at pH 7.8 because of which the carboxylic carbonyl of **1** appearing at 1718 cm^{-1} in FTIR of the multicomponent gel at pH 3.1 underwent bifurcation with reduced intensity as opposed to disappearing at pH 7.8 (Fig. S10, ESI†). Further addition of NaOH causes deprotonation of **2** and destroyed the salt-bridge as evident from the disappearance of the peaks near 1718 cm^{-1} at pH 10.4 (Fig. S10, ESI†). The NMR spectra show that, with a progressive increase of pH, the amides (H_a, H_b) and –CH protons of **1**, as well as the methylene protons (H_c) of **2**, underwent upfield chemical shifts gradually (Fig. S11, ESI†). The extent of upfield shifts of the protons were less compared to the case when the components were present alone with NaOH. At pH 7.8, the ammonium protons of **2** (H_d) were too broad to distinguish along with slight upfield shifts of the pyrene protons compared to the gel at pH 3.1, again suggesting salt bridge formation between the carboxylate of **1** and ammonium salt **2** at pH 7.8.[31]

The differences in the molecular-level interactions of the gels affect the aggregation depending on the pH. In the UV-vis spectra, the absorption at 325 nm and 341 nm for the multicomponent gel at pH 3.1 became broad at pH 7.8 with the emergence of a new band at 354 nm (Fig. S12, ESI†). In contrast, the binary gel at pH 10.4 had two distinct peaks at 334 nm and 350 nm. Different aggregation also influences the emission of the gels (Fig. S13, ESI†). On excitation of the naphthalene at 280 nm,[32] the hydrogel of **1** exhibited strong emission at 357 nm. In the multicomponent gel of (**1** + **2**) at pH 3.1, the naphthalene emission was quenched due to energy transfer from naphthalene to pyrene group.[33,34] Instead, a strong emission at 397 nm and a relatively less intensified band near 480 nm were predominant corresponding to the monomer and excimer emission of pyrene respectively. Normalization of the emission spectra revealed a gradual increase in relative intensity of the excimer band with the pH increase suggesting aromatic stacking plays a pivotal role in self-assembly at high pH.

We next performed the EDC coupling reaction with the multicomponent gels at pH 7.8 and 10.4 using a post gelation functionalization technique (Fig. S14 and S15, ESI†). ^{1}H NMR spectra of the EDC-treated gel at pH 7.8 (after freeze-drying) shows a downfield chemical shift (0.11 ppm) for the methylene protons of **2** (H_c) compared to the original gel. Moreover, simultaneous downfield shifts of the C-terminal –CH proton of **1** by 0.17 ppm indicates crosslinking between **1** and **2**; however, the newly formed amide bond (**3**, Fig. 3b) was not distinguishable due to overlapping with other signals. Similar trends in the NMR spectra were found for the EDC-treated gel at pH 10.4. Amide bond formation was confirmed by high-resolution mass spectrometry, which shows the expected mass for compound **3** at both pH 7.8 and 10.4 (Fig. S16, ESI†). From FTIR spectroscopy, the characteristic stretching signal for the –NH protons of **2** (H_d, Fig. 3) centered near 3280 cm^{-1} disappeared completely after treatment with EDC (Fig. 3a). Simultaneous emergence of a broad peak near 3400 cm^{-1} confirms the formation of amide **3**. Noticeably, the bifurcated signals near 1718 cm^{-1} attributed to salt-bridge between **1** and **2** at pH 7.8 also disappeared after amide bond formation.

Acidifying the samples showed disappearance of the peak at 8.57 ppm for –NHs of **2** (H_d) along with ~0.1 ppm upfield shifts of the pyrene H_e-proton (Fig. 3b and c) demonstrating the formation of crosslinking product **3** in both cases. Integration of the ^{1}H NMR spectra shows 82% and 88% conversion to amide **3** after 20 hours at pH 7.8 and 10.4 respectively. Again, the direct addition of EDC to the mixtures of **1** and **2** in presence of 1 and 2 equivalents of NaOH led to the identical proton NMR, further confirming that cross-linking is indeed taking place *via* amide bond formation (Fig. 3c and Fig. S15, S16, ESI†).

We monitored the effects of chemical crosslinking in the gels at pH 7.8 and 10.4 by rheology (Fig. 4a, b and Fig. S17, ESI†). Slow diffusion of EDC into the gels resulted in a gradual increase of both

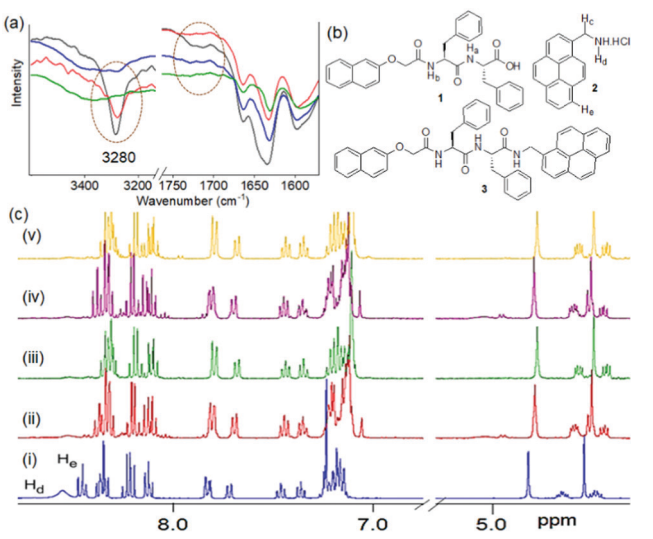

Fig. 3 (a) Changes in FTIR spectra of the gels of (**1** + **2**) at pH 7.8 (black) and 10.4 (red) after treatment with EDC (blue and green respectively). (b and c) Partial ^{1}H NMR spectra (in DMSO-d_6) spectra of the hydrogel of (**1** + **2**) at pH 3.1 (i) and the acidified samples of the EDC-treated gels (ii–v). For (ii) and (iii), EDC was added to the preformed gels (post assembly functionalization) of (**1** + **2**) at pH 7.8 and 10.4 respectively. For (iv) and (v), EDC was directly added to the mixture of (**1** + **2**) in presence of 1 equiv. and 2 equiv. amounts of NaOH respectively. For (ii–v), samples were acidified using HCl after ~20 h of addition of EDC and then freeze-dried. In all cases, initial concentration of **1** is 2 mg mL^{-1} and molar ratio of **1** and **2** is 1 : 1, concentration of EDC is 1 equivalent. Solvent is DMSO/H_2O (20/80, v/v).

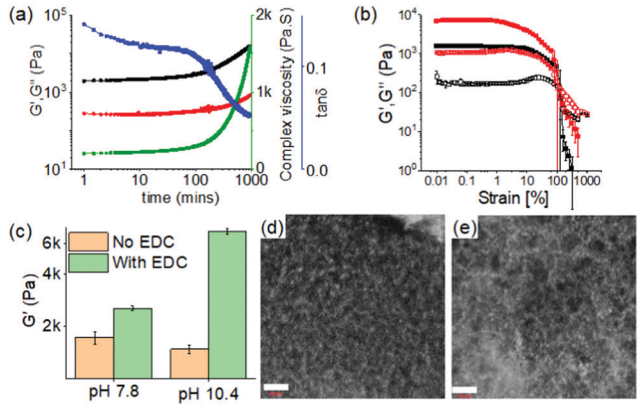

Fig. 4 (a) Variation of G' (black), G'' (red), complex viscosity (green) and tan δ (blue) with time for the hydrogels of (**1** + **2**) at pH 10.4 upon addition of EDC. (b) Strain sweeps of hydrogels of (**1** + **2**) obtained before (black) and after (red) addition of EDC at pH 10.4. (c) Bar graph showing the changes in stiffness (G', calculated at 0.5% strain from strain sweeps) of the multicomponent gels of (**1** + **2**) at pH 7.8 and 10.4 after crosslinking using EDC. (d and e) Confocal microscopy images (scale bars represent 20 μm) of the crosslinked hydrogels obtained at pH 7.8 and 10.4 respectively. In all cases, initial concentration of **1** is 2 mg mL^{-1} and molar ratio of **1**, **2** and EDC is 1 : 1 : 1. Solvent is DMSO/H_2O (20/80, v/v).

complex viscosity and rheological moduli (G' and G'') over time corroborating crosslinking-driven evolution to a stiffer material at both pH. A concomitant reduction in the value of tan δ (G''/G') further implies an increase in the solid-like nature of the gels. We highlight that crosslinking between **1** and **2** is possible between the adjacent fibres or between the components present in the same fibres. The crosslinked gel formed at pH 10.4 was found to be mechanically stiffer (~3 fold higher G') than the crosslinked gel at pH 7.8 (Fig. 4c and Fig. S17, ESI†). The newly formed amide bond contributes to establishing stronger intermolecular interaction between the molecules that increased the mechanical properties of the gels. Compared to the pristine gels of (1 + 2), the mechanical stiffness of the crosslinked gels increased by ~2 fold and ~5 fold at pH 7.8 and 10.4 respectively (Fig. 4c). However, under confocal microscope, both the crosslinked gels revealed identical microstructures with a substantial increase in the density of spherulitic domains than the original materials (without EDC) (Fig. 4d and e). There was also a slight change in the absorption spectra of the crosslinked gels (Fig. S18, ESI†). In both cases, the peak at 334 nm was predominant along with a broad shoulder peak near 320 nm. At both the pH, crosslinking resulted in a gradual decrease of both the monomer and excimer emission of pyrene with practically almost quenching of the monomer emission (at 397 nm) at pH 10.4 (Fig. S19 and S20, ESI†). Correlation of normalized emission spectra with FTIR of the EDC-treated gels implies that in association with intermolecular hydrogen bonding, aromatic stacking further contributes to the mechanical properties of the crosslinked gel at pH 10.4, as can be seen from the rheology data. As the conversion to the amide **3** at both pH 7.8 and 10.4 was almost same, indicating that the differences in rheological properties of the gels were primarily due to change in molecular packing of **3** at different pH. Interestingly, we obtained gels with the freeze-dried samples of the EDC treated gels at pH 7.8 and 10.4 indicating that the crosslinking product **3** could behave as a gelator by its own. However, the visual appearance and mechanical properties of these gels are very different from the directly obtained EDC treated gel (*in situ* formation of **3**) (Fig. S21 and S22, ESI†) presumably due to the change in preparative pathway and showing that *in situ* crosslinking results in a different material than in 3 is used directly as a gelator.

Overall, we have shown that with appropriate gelator design, hydrolysis of EDC can be used to achieve a permanent covalent cross-linking through amide bond formation between the components in a multicomponent gel. Unlike traditional EDC-fueled systems where transient covalent crosslinking leads to materials with a short lifetime[24–26] potentially imposing limitations on their practical applications, our method allows preparing crosslinked gels with enhanced mechanical properties. The ability of pH-responsive charge complementary multicomponent systems to achieve different degrees of ionization upon pH change provides a further level of control on the final stiffness of the materials. Beyond the conventional methods of covalent crosslinking, our approach would be more promising as a library of multicomponent gels can be derived by simple mixing of gelators with carboxylic acid and amine groups.[18–20]

SP thanks the University of Glasgow for funding. We thank Lisa Thomson, Libby Marshall, and Simona Bianco for their help with the NMR experiments.

Conflicts of interest

There are no conflicts to declare.

Notes and references

1 D. B. Amabilino, *et al.*, *Chem. Soc. Rev.*, 2017, **46**, 2404.
2 P. Terech, *et al.*, *Chem. Rev.*, 1997, **97**, 3133.
3 X. Du, *et al.*, *Chem. Rev.*, 2015, **115**, 13165.
4 J. Li, *et al.*, *Soft Matter*, 2019, **15**, 1704.
5 Q. Peng, *et al.*, *InfoMat*, 2020, **2**, 843.
6 R. Boddula and S. P. Singh, *J. Mater. Chem. C*, 2021, **9**, 12462.
7 D. J. Cornwell and D. K. Smith, *Mater. Horiz.*, 2015, **2**, 279.
8 J. Wang, *et al.*, *J. Mater. Chem.*, 2009, **19**, 7892.
9 D. A. Stone, *et al.*, *Soft Matter*, 2011, **7**, 2449.
10 S. Panja and D. J. Adams, *Chem. Soc. Rev.*, 2021, **50**, 5165.
11 Y. Ding, *et al.*, *Langmuir*, 2013, **29**, 13299.
12 E. R. Draper, *et al.*, *Chem. Commun.*, 2015, **51**, 12827.
13 M. N. Tahir, *et al.*, *Polym. Chem.*, 2018, **9**, 3019.
14 L. Aulisa, *et al.*, *Biomacromolecules*, 2009, **10**, 2694.
15 M. A. Khalily, *et al.*, *Org. Biomol. Chem.*, 2015, **13**, 1983.
16 L. Chronopoulou, *et al.*, *N Biotechnol.*, 2017, **37**, 138.
17 W. Edwards and D. K. Smith, *J. Am. Chem. Soc.*, 2014, **136**, 1116.
18 D. M. Raymond and B. L. Nilsson, *Chem. Soc. Rev.*, 2018, **47**, 3659.
19 B. O. Okesola and A. Mata, *Chem. Soc. Rev.*, 2018, **47**, 3721.
20 L. Li, R. Sun and R. Zheng, *Mater. Des.*, 2021, **197**, 109209.
21 B. Rieß, *et al.*, *Chem*, 2020, **6**, 552.
22 G. Wang and S. Liu, *ChemSystemsChem*, 2020, **2**, e1900046.
23 P. S. Schwarz, *et al.*, *Chem. Commun.*, 2022, **58**, 1284.
24 J. Heckel, *et al.*, *Angew. Chem., Int. Ed.*, 2021, **60**, 7117.
25 B. Zhang, *et al.*, *Chem. Commun.*, 2019, **55**, 2086.
26 O. J. Dodo, *et al.*, *Macromolecules*, 2021, **54**, 9860.
27 S. Panja and D. J. Adams, *Chem. Commun.*, 2019, **55**, 10154.
28 Y. Cho, *et al.*, *Nat. Commun.*, 2021, **12**, 7340.
29 C. Redondo-Gómez, *et al.*, *Biomacromolecules*, 2019, **20**, 2276.
30 M. Tena-Solsona, *et al.*, *J. Mater. Chem. B.*, 2014, **2**, 6192.
31 P. Chakraborty, *et al.*, *Chem. Commun.*, 2020, **56**, 5251.
32 L. Chen, *et al.*, *Chem. Commun.*, 2010, **46**, 4267.
33 S. Nandi, *et al.*, *J. Mol. Recognit.*, 2016, **29**, 303.
34 P. Rajdev and S. Ghosh, *J. Phys. Chem. B*, 2019, **123**, 327.